# GOME-1 Level 1 Version 5 Radiance Validation

**Kai-Uwe Eichmann, Mark Weber, and John P. Burrows**
Institut für Umweltphysik, Universität Bremen, Bremen, Germany

| | | |
|---|---|---|
| Document Number | : | gome1 lv1 rad val v1.0 |
| Version | : | 1.0 |
| Date | : | November 29, 2017 |
| Contact | : | Kai-Uwe Eichmann (eichmann@uni-bremen.de)<br>Universität Bremen FB1<br>P.O. Box 330 440<br>D-28334 Bremen |
| Status | : | first draft |

# Contents

# 1 Introduction

The GOME-1 (Global Ozone Monitoring Experiment) on ERS-2 was launched in April 1995 to provide nadir radiance measurements for the retrieval of trace gases, mainly ozone. It measured in the spectral region from 237 to 794 nm in four channels with a spectral resolution of 0.2–0.4 nm (Burrows et al., 1999). Channel 1A detects photons in the spectral range of 237–282 nm with an on detector chip integration time (IT) of 12 s. Channels 1B and 2A/B measure in the spectral range of 282–314 nm and 311–405 nm, respectively, mainly with IT=1.5 s. The IT of 1B was changed from 12 s to 1.5 s on 7 June 1998. The spectral ranges (IT=1.5 s) of channels 3 and 4 are 394–610 nm and 578–794 nm, respectively.

GOME-1 has measured in forward and backward scan-mode. In the forward mode, three ground pixels of usually 40 km by 320 km were measured across-track while the back-scan covers 40 km by 960 km. Thus, the spatial resolution of one forward scan ground pixel is 40 km by 320 km for channels with an integration time of 1.5 s and about 100 km (80 km-120 km) by 960 km (6 forward scan ground pixels and 2 back-scan ground pixels) for channels with an integration time of 12 s. GOME provides global coverage at the equator within 3 days. After the failure of the tape recorder on ERS-2 in June 2003, global coverage could no longer be achieved. The GOME instrument ceased its operation in the middle of 2011.

This report focuses on the verification of the version 5 Level-1 spectra in the UV range (285–355 nm) and the visible range (545–565 nm and 649–669 nm). This study is an update of the study by Boetel, Weber, and Burrows (2016) using the new complete version 5 GOME-1 dataset. We used radiances computed with the radiative transfer model SCIATRAN in the UV wavelength range for selected regions to compare with the GOME-1 radiances. Then monthly and annual mean ratios were derived.

It can not expected that these two radiance datasets fully agree, taking into account the imperfect knowledge of the real atmospheric state and surface boundary conditions, needed as input for the RTM. But nevertheless, the RTM radiance dataset can act as an anchor over time, as there is no degradation possible.

Comparisons with ATSR-2 reflectivities are performed for the visible wavelength range (555 and 660 nm). The GOME-1 radiances are therefore converted to reflectivities using the visible ATSR-2 spectral response functions. The spatially highly resolved ATSR-2 reflectivities were downgraded by averaging over the GOME-1 pixel size.

# 2 Available datasets

## 2.1 ESA GOME-1 L1V5 radiances

The new ESA/DLR operational GOME-1 level 1 version 5 dataset was used for this study. The data are stored in netCdf format and were processed using IDL H5 extraction routines. We extracted all radiances with an IT=1.5 sec. That means that the wavelengths below 307 nm are only available after the change of IT in channel 1B in 7 June 1998. The detection of cloud free measurements is restricted to the smaller pixel size.

## 2.2 ESA ATSR-2 GRAPE 3.2 reflectivities

The ATSR-2 reflectivities are taken from the GRAPE (Global retrieval of ATSR cloud parameters and evaluation) dataset. This product has a degraded pixel size in order to reduce data volume. The

GRAPE processing uses a super-pixel of 4 pixels along track and 3 pixels across track, so that the input dataset has 191 super-pixels across-track (Dean and Poulsen, 2007). The data is conveniently stored in HDF format and available for the time span of the GOME-1 comparison period from 1995–2003.

The GRAPE version 3.2 dataset is generated with the Oxford-Rutherford Appleton Laboratory (RAL) Aerosol and Clouds (ORAC) algorithm and provides Level-2 retrievals of cloud and aerosol properties from measurements of the Along-Track Scanning Radiometer (ATSR) family (Sayer et al., 2011). The cloud infrared (IR) brightness temperature as observed by ATSR-2 (Poulsen et al., 2011) is used in the GRAPE project. Cloud properties retrieved by GOME-1 and ATSR-2 have already been compared by Lelli et al. (2012).

The reflectances of ATSR-2 are averaged over the larger GOME-1 pixels, because of the pixel size differences between both instruments. On average, more than 500 ATSR super pixel are used for the spatial averaging. The GOME-1 radiances are convoluted with the radiance response functions of ATSR-2 which are shown in Fig. 1. The data can be downloaded from the ATSR website (www.atsr.rl.ac.uk/documentation/docs/filterfunctions/). No ATSR-2 data is available in the first half of 1996, due to a temporary scan mirror failure.

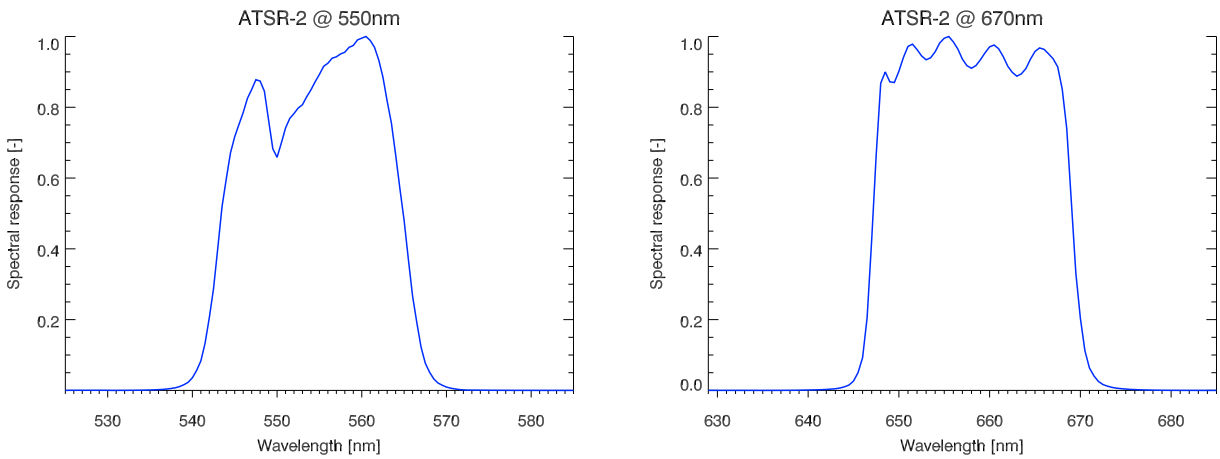


Figure 1: The ATSR operational level 1 radiance response functions in the visible wavelength range around 0.55 and 0.67$\mu$ used for the GOME-1 radiance convolution.

## 2.3 IUP SCIATRAN 3.6.4 radiances

The radiative transfer model SCIATRAN version 3.6.4 (Rozanov et al., 2014) was used to compute the radiances for the comparisons. The SCIATRAN model was initialized as follows:

- Date, time, and geolocation from the GOME-1 measurement pixel.
- Observation geometry for the middle of the integration time (sun zenith angle, relative azimuth angle, viewing zenith angle).
- The GOME-1 wavelength grid is used between 283 and 355 nm.
- Co-located pressure and temperature profiles using ECWMF ERA-interim data (Dee et al., 2011).

- Standard profiles for trace gases depending on latitude and month. $NO_2$, ClO, and BrO absorption spectra with climatogical profiles are taken into account.
- Adjusted ozone profiles from the IUP ozone climatology (Lamsal et al., 2004) are supplied using WFDOAS total ozone columns (Coldewey-Egbers et al., 2005; Weber et al., 2005) from co-located GOME-1 measurements. These are based on GOME-1 level 1 version 4 data.
- The vacuum GOME FM ozone cross sections have been used.
- The effective albedo is calculated from tabulated values of the LER (Lambertian Equivalent Reflectivity) using GOME-1 viewing geometry angles, the GOME-1 reflectivity at 377.63 nm, and the scene height. The surface is a Lambertian reflector.
- The aerosol content is taken to be constant with an optical thickness at 550 nm of 0.4. The scattering function is constructed using the Henyey-Greenstein parametrization.
- The GOME-1 instantaneous field of view of 0.14 is used.
- Sun-glint affected measurements of GOME-1 are excluded.

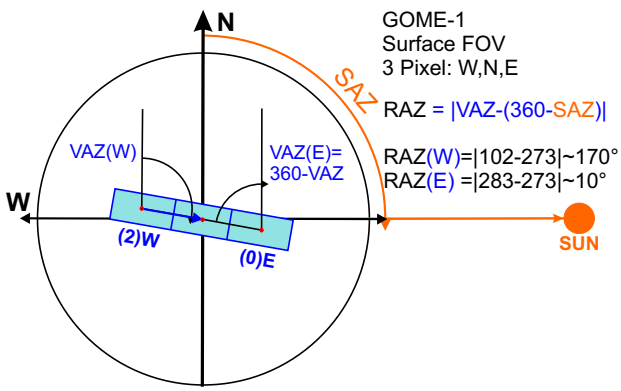


Figure 2: The azimuthal viewing geometry, as defined for GOME-1. The three ground scenes are shown.

The relative azimuth angle RAZ is calculated as the angle between the solar and the viewing azimuth direction. The sun azimuth is defined where the instruments line-of-sight crosses the surface as the angle between the North and the solar viewing direction. The viewing azimuth angles is defined similarly as the angle between the North and the Nadir viewing direction. For SCIATRAN, the RAZ must be zero, when the instrument is looking towards the sun. Thus lowest RAZ are computed for the Eastern pixel of GOME-1. The geometry is summarized in Fig. 2

# 3 Method of comparisons

## 3.1 Comparison of GOME-1 and SCIATRAN UV radiances

The UV radiances are compared to SCIATRAN sun-normalized radiances. The GOME-1 measurements are only used for scenes of really low cloud fractions (CF$<$0.09) to avoid larger errors due to broken cloud fields in the field of view. Four regions are chosen, both over bright surfaces (deserts,

Antarctic continent) and dark surfaces (oceans). The differences are then averaged per month to make the time series. The box boundaries for the five regions are shown in Fig. 3: Tropical Pacific (23S-23N, 180-220E), Northern desert (15-30N, 0-25E), Southern desert (30-20S, 120-135E), Antarctic (80-70S, 0-360E).

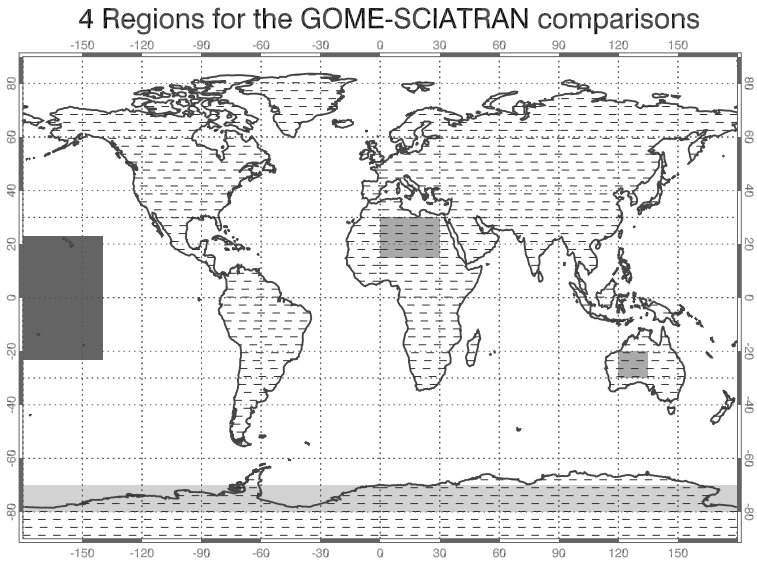


Figure 3: The four regions where the GOME-1 measurements are sampled for the SCIATRAN comparisons.

SCIATRAN calculates radiances for an incident solar radiation of 1. That is the same as dividing the measured GOME-1 radiance $R_G$ with the corresponding solar irradiance $I_G$. The absolute ratio $r_a$ is then defined as:

$$r_a(\lambda) = \frac{R_G}{I_G R_S}, \tag{1}$$

where $R_S$ is the sun normalized SCIATRAN radiance. The initial calibration correction $r_0$ is done for the first 2 months of measurements right after launch. We only show the monthly calibration correction $c_m$, which is:

$$c_m(\lambda) = \frac{r_a}{r_0}. \tag{2}$$

This is done for all data of the collected regions. To increase the speed of calculations, only every fifth GOME-1 wavelength was computed to get SCIATRAN radiances. The absorption cross sections of ozone were degraded accordingly with a 5 point triangular smoothing. This was also applied to the GOME-1 sun normalized radiances. It was thus possible to calculate SCIATRAN model radiances for the full GOME-1 dataset within a week. Comparisons between the original wavelength grid and the reduced one has shown that the differences of the corresponding correction factors are negligible with respect to the overall biases of the method. Differences of $c_m$ are less than 1% for all wavelength bands.

Figure 4 shows an example of the ratio $r(\lambda)$ for the original data and 2 steps of averaging. For simplicity, we used the 10 nm averaged data (red diamonds) for the monthly averaging and all wavelengths only for the annual means.

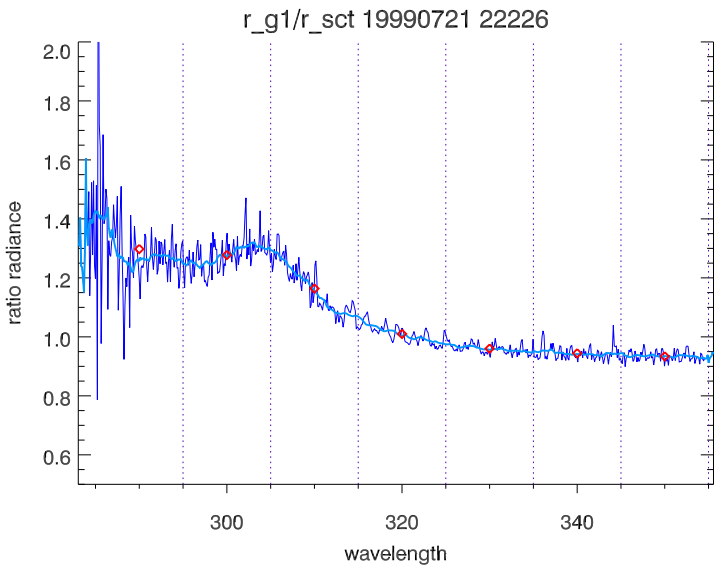


Figure 4: The ratio of GOME-1 and SCIATRAN for one pixel (1999/07/21, orbit 22226, state 3). The high resolution original data is superimposed by the 2 nm smoothed ratio (light blue) and the 10 nm averaged values (red diamonds), as used in this study.

### 3.2 Comparison of visible GOME-1 and ATSR-2 radiances

The ATSR-2 radiances are measured for very small ground pixel sizes in the order of 1x1 km$^2$. We are using a horizontally degraded dataset of 3x4 km$^2$ taken from the GRAPE project. The radiances of GOME-1 are convoluted with the spectral response functions of ATSR-2 and the pixel size of ATSR-2 is averaged for all pixel lying inside the GOME-1 pixel. To reduce the amount of data and to minimize mixing effects of broken cloud fields, the GOME-1 cloud fractions are used. The maximum cloud fraction for the GOME-1 pixel is taken as 0.1, similar to the UV calculations. The averaged ATSR-2 reflectivities will nevertheless be contaminated with pixels of higher cloud fraction. This will enhance the ATSR-2 reflectivity scatter (standard deviation). Currently, the scatter is stored, but not taken into account in these comparisons.

The ATSR-2 normalised response functions ranges from 525 nm to 585 nm and from 629 nm to 685 nm with a resolution of 0.5 nm as shown in Fig. 1. The response was linearly interpolated to the GOME-1 wavelengths. Both the irradiance and radiance of GOME-1 was integrated using the response function to get the GOME-1 adjusted radiances $< r_G(ATSR) >$ and irradiance $< i_G(ATSR) >$. The GOME-1 reflectivities are then calculated as:

$$ref_G(i) = \frac{< r_G(ATSR) >}{< i_G(ATSR) > cos(SZA)}. \quad (3)$$

The ATSR-2 reflectivities are averaged by using all ATSR-2 measurements where the latitude/longitude centre pixel is inside the larger GOME-1 pixel. Roughly 500-1000 ATSR-2 pixels can be found per one GOME-1 pixel.

# 4 Results

## 4.1 The L1V5 dataset in the UV

The dataset of GOME-1 radiances stored in netCDF format comprises among the geolocation and geometry angles also the cloud fraction, which is needed to reduce the data volume and improve the comparability with SCIATRAN radiances. Partly cloudy scenes should be avoided as they can not be modelled exactly in a radiative transfer model. The number of measurements that are available per month for the three across track angles with cloud fraction less than 0.09 is in the order of 100–600 measurements. For the period of June to October 1998 and in February 2001 less than 100 data points were found. No measurements with adequate cloud fraction were extractable after June 2003.

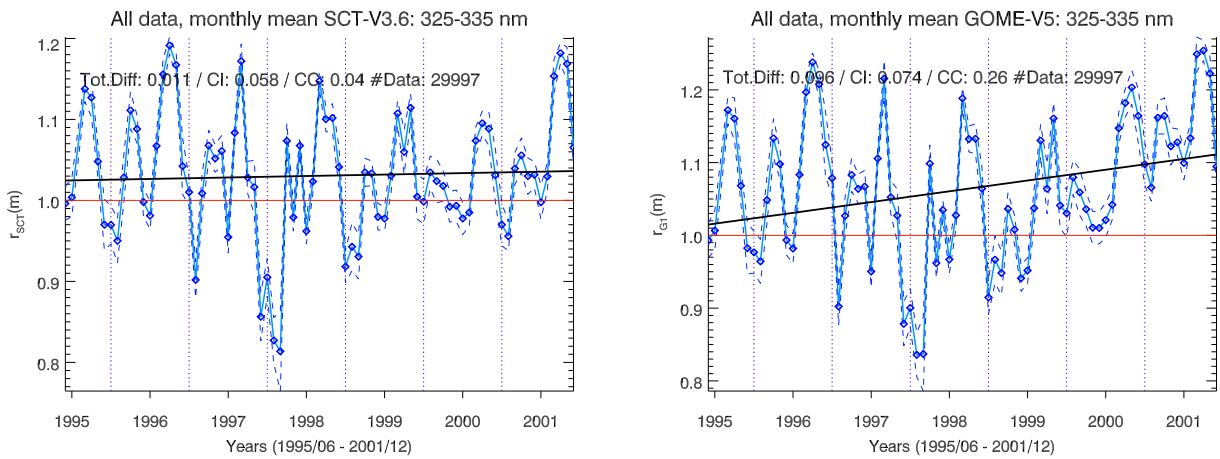


Figure 5: The evolution of GOME-1 V5 (right) and SCIATRAN V3.6 (left) radiances as a function of time for the 325-335 nm band. The radiances are normalized by the averaged first two months of data.

The comparisons with SCIATRAN are done for 4 regions and 7 wavelength bands of 10 nm between 285 nm and 355 nm. No data is available for the first two bands of 285-295 nm and 295-305 nm until June 1998 due to integration time differences. To check the general behaviour of the two dataset to compare, normalised radiance of SCIATRAN and GOME-1 are plotted in Fig. 5. Despite the intra-annual variance, SCIATRAN shows the more constant behaviour over time. This is expected, as the RTM is driven by independent atmospheric parameters and no degradation will influence the radiances.

When combining all available data for the 4 regions, we get rather stable time dependencies of the correction factor. Figure 6 shows an example of the monthly calibration correction factors (CCF) for the 325-335 nm band. The absolute CCF is divided by the average of the CCF from the first 5 weeks in June/July 1995. The time span is from June 1995 to June 2003. The variance of CCF is roughly within $\pm$4% until the middle of 2000, where a larger increase up to 15% is detected. This is only temporary and at the end of 2001, no difference was detected. For the last 18 months until the end of the comparison time frame, GOME-1 values decrease by about 5% with respect to the model. The overall standard deviation of $c_m$, shown as dashed blue lines, is in the order of 0.05.

A trend analysis using the robust Theil-Sen regression (Sen, 1968) with Spearman correlation coefficient (CC) show an insignificant trend for the whole time series. The difference between both values is about 2% , the total trend of about -0.007 (-0.7% ) over the whole time is within the range of the confidence interval (CI) of 0.3 with a CC of -0.09. Overall, about 35000 measurements and

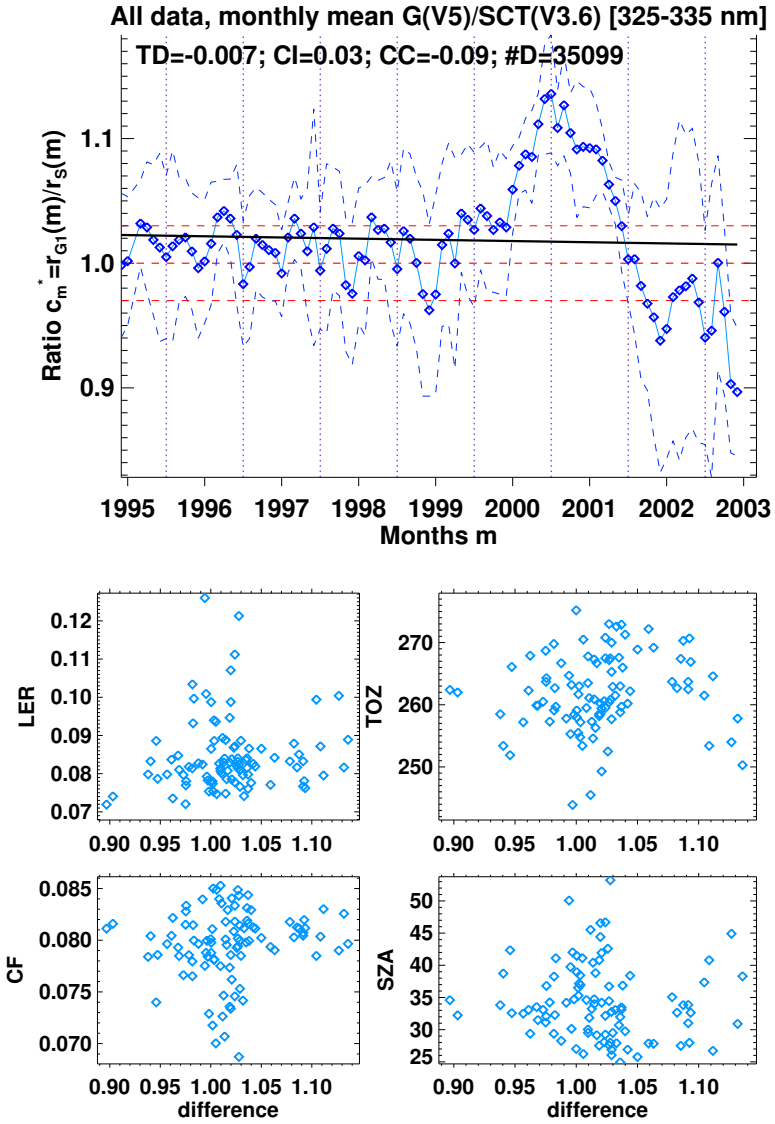


Figure 6: The monthly calibration correction $c_m$ and the trend from GOME-1 V5 and SCIATRAN V3.6 radiances as a function of time for the 325-335 nm band (top). The data was gathered for the four regions. Scatter plots (bottom) of the radiance ratio versus various input parameters used in the SCIATRAN calculations: LER (top left), total ozone (top right), cloud fraction (bottom left), and sun zenith angle (bottom right).

radiative transfer calculations were used.

The scatter plots show no dependencies of the correction factor with respect to the relevant input parameters. We deduce that the calibration of the new level 1 radiances is good for most of the measurement time frame. Naturally, large differences between SCIATRAN and measurements can occur as not all atmospheric parameters are accounted for in the model. For example, aerosols intrusions due to volcanic events can add a significant amount of additional scatterers into the upper troposphere/lower stratosphere. Also, the remaining clouds in the field of view can lead additional changes of the CCF.

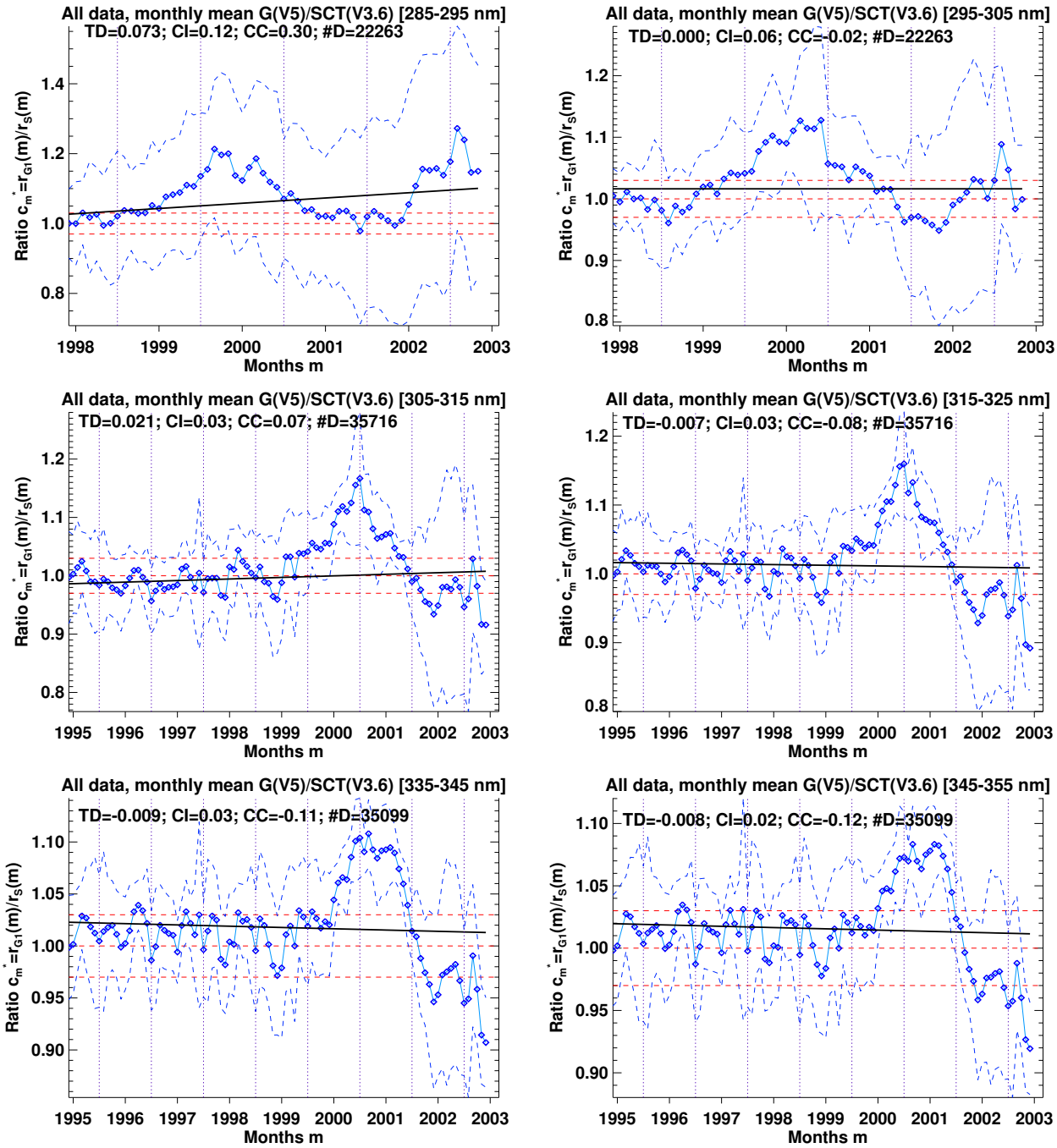


Figure 7: Comparison of GOME-1 V5 and SCIATRAN V3.6 monthly mean radiances using all four regions for all wavelength bands. Please note the different time periods for the first two bands.

Fig. 8 shows the trend analysis for 6 bands from 285 to 355 nm. About 35000 SCIATRAN calculations were performed for the comparisons. No significant trends were found for all wavelength bands and the corrections factors are within 5% for most of the months. Similar features are seen here again with the increase in 2001 and the decline towards the end of the comparison period.

The first two bands between 285 nm and 305 nm are in the channel 1B and comparisons were only made for IT=1.5 sec. Thus, only after June 1998 comparisons were possible that are shown here. The 300 nm band comparisons are similar to the other bands. But the 290 nm band shows an increase in GOME-1 radiances over time even in the period of 2002/2003.

The calibration of the new level 1 version 5 GOME-1 radiances is best between 1995 and the middle of 2000, when compared to the adjusted radiative transfer model SCIATRAN. After that long period, the bias increases. After the failure of several on-board gyro systems in 2001, the ERS-2 flew in a "gyro-less" yaw steering mode. A failure in the on-board data storage system in 2003 meant for GOME-1 that science data was directly relayed to ground at the time of acquisition. Less measurements per day were downlinked. No usable GOME-1 measurements for the selected regions were found after July 2003.

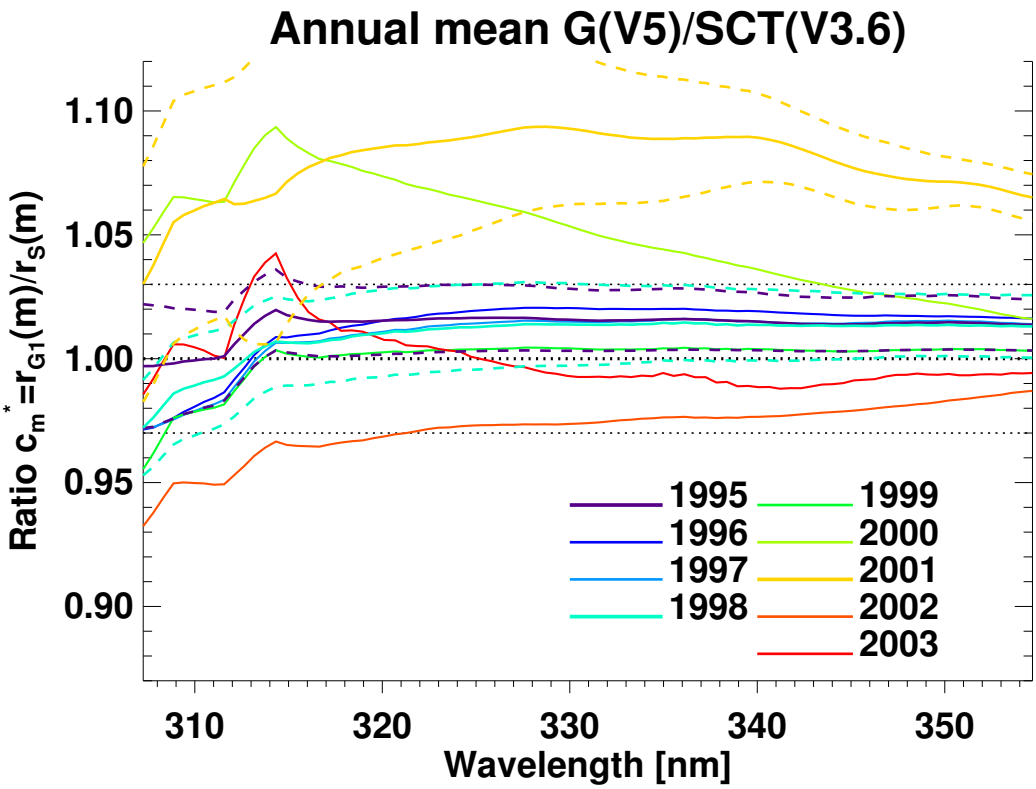


Figure 8: Comparison of GOME-1 V5 and SCIATRAN V3.6 annual mean radiances of all four regions. Overplotted is the line at one and the 3% range. The standard deviation is also shown for the years 1995 (violet), 1998 (light blue), and 2001 (yellow).

To make the results comparable with the last report, we also made annual means for the full wavelength range between 305 and 355 nm. The data was smoothed using a 5 point boxcar. The differences over all wavelengths are within $\pm$2% for most of the years, except for 2000, 2001, and 2002. The largest difference up to 9% was found for 2001, where GOME-1 radiances were higher and in 2002 down to -6% for the GOME-1 radiances.

## 4.2 The L1V5 dataset in the visible

We calculated the ratio [%] of GOME-1 versus ATSR-2 reflectivities for cloud fraction from GOME-1 below 0.1 to reduce the amount of data. These were then averaged for each year to check the global distribution and the corresponding standard deviation. An example for the 550 nm band is shown in Fig. 9 for 1999. The data is binned into 10 times 10 deg boxes.

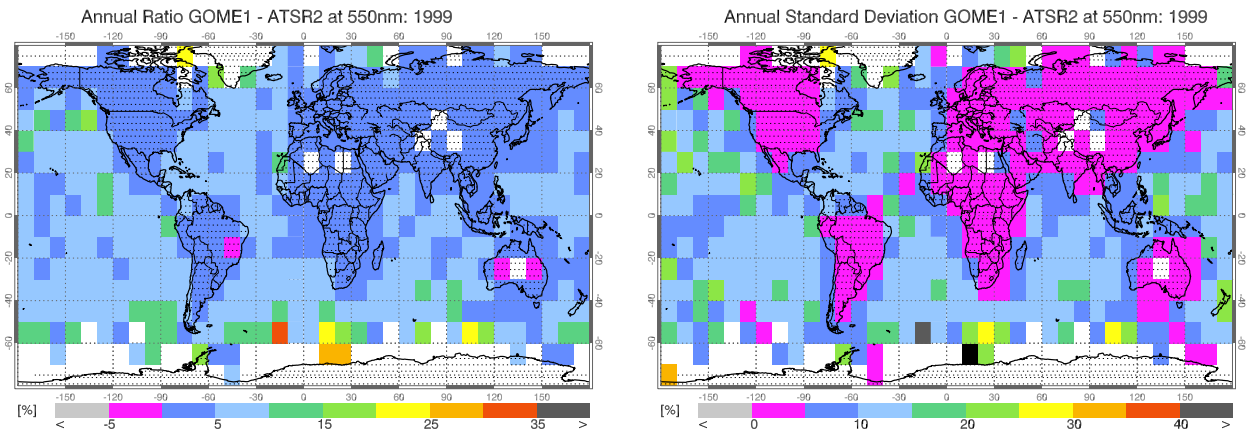


Figure 9: The annual mean of the 550 nm band GOME-1 / ATSR-2 ratio [%] for the year 1999 (left) and the corresponding standard deviation (right). The grid box size is 10deg in latitude/longitude direction.

The average difference between both dataset is globally nearly uniform and in the order of 4% with higher values towards the poles. A slight change of the level of difference is detectable between ocean and land. This difference is more pronounced when taking the standard deviation (SD) into account, which is clearly lower over land ($< 5\%$) than over oceans ($< 20\%$).

The zonally, monthly mean ATSR-2 and GOME-1 reflectivities for both visible wavelength bands are shown as a function of time and latitude in Fig. 10. There was a data gap of ATSR-2 data at the beginning of 1996. Between 1995 and 2000, the two reflectivities compare quite nicely. GOME-1 $ref_G$ in the first two months of 1997 are unusually high. We have not reduced the GOME-1 data for instrumental artefacts, e.g., temperature instabilities. While the GOME-1 reflectivities remain stable over time, the ATSR-2 $ref_A$ starts decreasing in 2001 in both bands. We extended the period of comparisons up to July 2003 to check if this an ongoing phenomenon. The ATSR-2 change of reflectivity in the visible wavelength bands in the GRAPE dataset is a known feature. After the start of the no-gyro Attitude and Orbit Control System (AOCS) modes on 16 January 2001, the product quality is regarded as unacceptable (ESA, 2015).

The ratio of GOME-1 versus ATSR-2 averaged reflectivities shown in Fig. 11 covers the full time span available up to July 2003. After the beginning of 2001, the comparisons show larger differences due to a decrease in the ATSR-2 reflectivities as seen in Fig. 10. Thus, the comparisons are not useful after 2000. For the earlier period, both instruments agree with a slight bias of less than 10% , with GOME-1 reflectivities being higher for all latitude bands.

A trend analysis using the robust Theil-Sen regression (Sen, 1968) with Spearman correlation coefficients show small trends in the differences as shown in Fig. 12. The correlation coefficients are very low (about 0.22) for both latitude bands and the confidence intervals are in the range of the total trends of 5%. The differences can be attributed to the ATSR-2 dataset (see Fig. 10). Except for this outlier, the two datasets are relatively similar with the GOME-1 reflectivities being higher by about

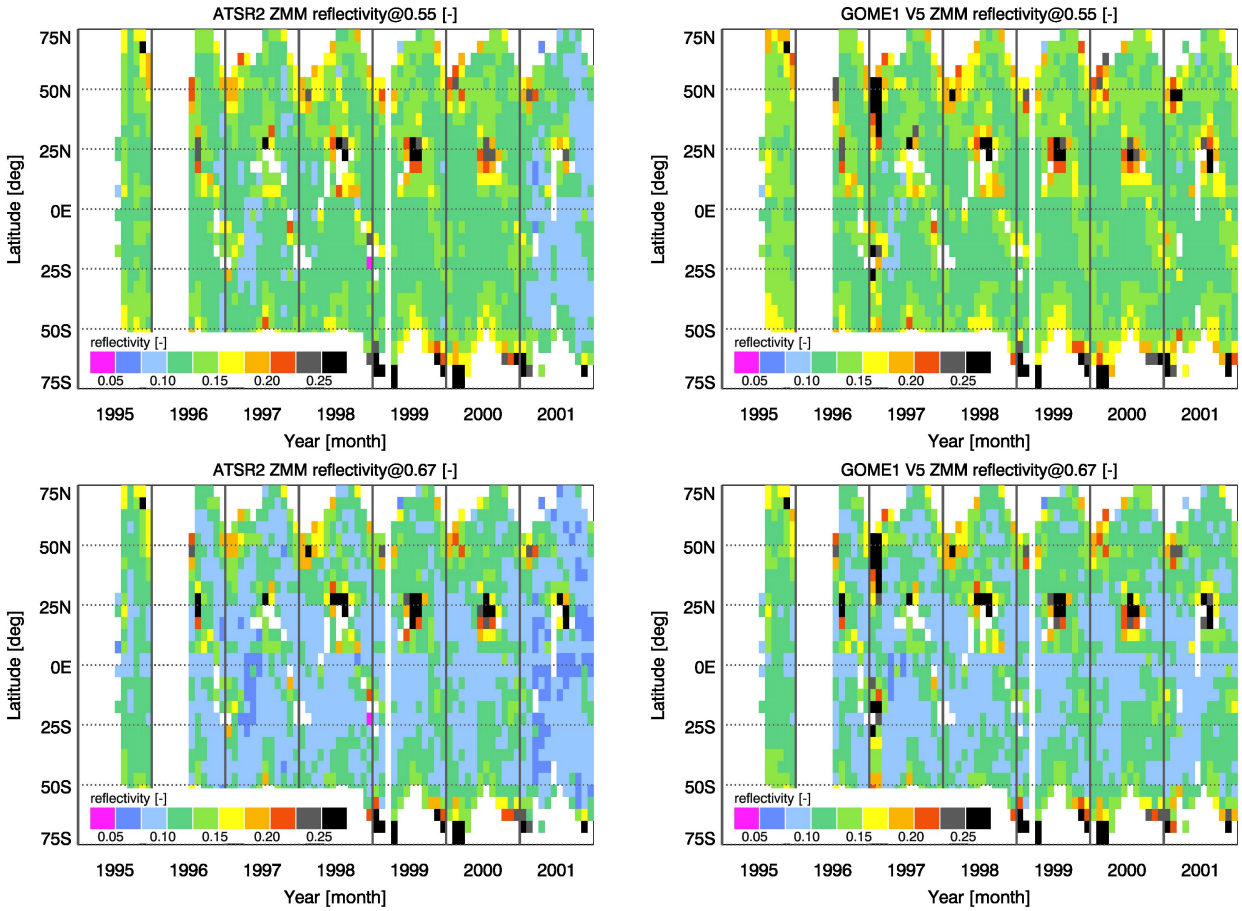


Figure 10: The zonally averaged ATSR-2 (left) and (right) GOME-1 reflectivities for the visible channels 550 nm (top) and 670 nm (bottom) as a function of time and latitude.

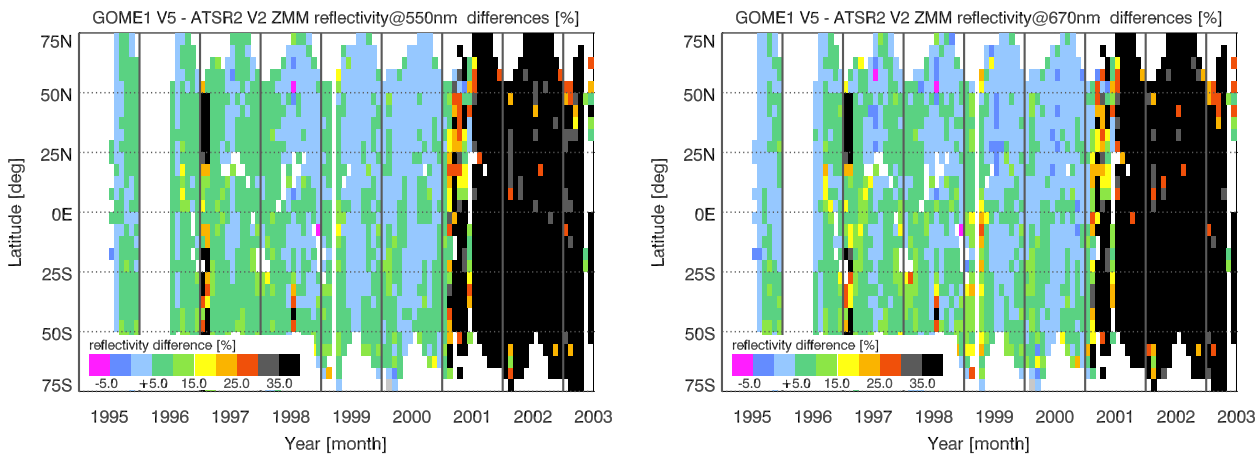


Figure 11: The zonally averaged reflectance differences of ATSR-2 versus GOME-1 for the two visible channels as a function of time.

5%. The total increase over the time span is dependent on the latitude band and in the order of less

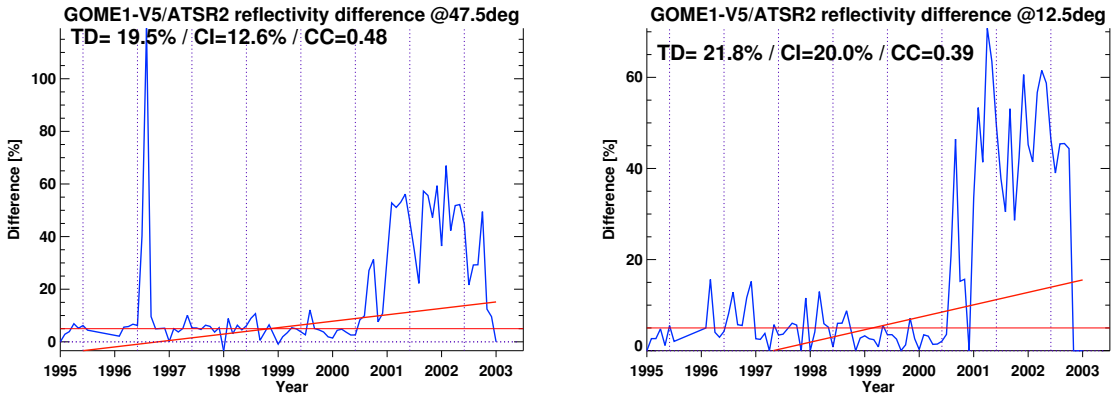


Figure 12: Trend analysis (Theil-Sen) of GOME-1 / ATSR-2 differences [%] of the 670 nm band for the latitude bands 45-50 deg and 10-15 deg North.

than 5%. This is driven by the largest differences in 2001-2003. The confidence interval is generally larger than the increase.

# 5 Summary

The main findings for the GOME-1 level 1 version 5 radiances are:

- Using all data available for cloud fractions less than 0.09, the GOME-1 and SCIATRAN radiances compare very well. The temporal evolution is rather constant. The Theil-Sen regression analysis showed that the average radiance difference is in the order of less than 3% for all bands except 285-293 nm. Also, no significant trend was detected.
- The annual mean calibration correction factors show no wavelength dependent features for the first 5 years of data with biases of less than 3%. After ERS-2 problems with stability in 2001, larger differences were found with higher GOME-1 radiances in 2000 and 2001.
- Due to the change of IT in channel 1B in 7 June 1998, radiances below 307 nm are only available after 7 June 1998 with an IT=1.5s. The first 2 bands below 305 nm can thus only be checked after that date. The 300 nm band is similar to the higher bands. But the 290 nm band exhibits an increase in the GOME/SCIATRAN radiance ratio of about 7% which is nevertheless within the uncertainty of the method and statistically not significant.
- After the loss of the tape recorder in June 2003, no data are available for the selected regions.
- The ATSR-2 comparisons show no significant trends. The differences are in the order of 5% with a general uncertainty of less than $\pm$15% . The ATSR-2 radiances in the GRAPE dataset started to decrease due to the no-gyro Attitude and Orbit Control System (AOCS) modes starting on 16 January 2001 (ESA, 2015), when the ATSR-2 GRAPE data was not usable any more.

# 6 References

Boetel, S., Weber, M., and Burrows, J. P.: GOME Level-1 V5 Verification, Technical note, Institute of Environmental Physics, University of Bremen, 2016.

Burrows, J. P., Weber, M., Buchwitz, M., Rozanov, V. V., Ladstätter-Weißenmayer, A., Richter, A., DeBeek, R., Hoogen, R., Bramstedt, K., Eichmann, K.-U., Eisinger, M., and Perner, D.: The global ozone monitoring experiment (GOME): Mission concept and first scientific results, J. Atmos. Sci., 56, 151–175, 1999.

Coldewey-Egbers, M., Weber, M., Lamsal, L. N., de Beek, R., Buchwitz, M., and Burrows, J. P.: Total ozone retrieval from GOME UV spectral data using the weighting function DOAS approach, Atmos. Chem. Phys., 5, 1015–1025, 2005.

Dean, S. and Poulsen, C. A.: Processed ATSR-2/AATSR data for the production of GRAPE (1995-2009), 2007.

Dee, D. P., Uppala, S. M., Simmons, A. J., Berrisford, P., Poli, P., Kobayashi, S., Andrae, U., Balmaseda, M. A., Balsamo, G., Bauer, P., Bechtold, P., Beljaars, A. C. M., van de Berg, L., Bidlot, J., Bormann, N., Delsol, C., Dragani, R., Fuentes, M., Geer, A. J., Haimberger, L., Healy, S. B., Hersbach, H., Hólm, E. V., Isaksen, L., Kållberg, P., Köhler, M., Matricardi, M., McNally, A. P., Monge-Sanz, B. M., Morcrette, J.-J., Park, B.-K., Peubey, C., de Rosnay, P., Tavolato, C., Thépaut, J.-N., and Vitart, F.: The ERA-Interim reanalysis: configuration and performance of the data assimilation system, Quart. J. R. Met. Soc., 137, 553–597, 2011.

ESA: ATSR-2 in the ERS-2 Post Gyro Failure Period, Technical note 1, ESA, 2015.

Lamsal, L. N., Weber, M., Tellmann, S., and Burrows, J. P.: Ozone column classified climatology of ozone and temperature profiles based on ozonesonde and satellite data, J. Geophys. Res., 109, 2004.

Lelli, L., Kokhanovsky, A. A., Rozanov, V. V., Vountas, M., Sayer, A. M., and Burrows, J. P.: Seven years of global retrieval of cloud properties using space-borne data of GOME, Atmos. Meas. Tech., 5, 1551–1570, doi:10.5194/amt-5-1551-2012, 2012.

Poulsen, C. A., Watts, P. D., Thomas, G. E., Sayer, A. M., Siddans, R., and Grainger, R. G.: Cloud retrievals from satellite data using optimal estimation: evaluation and application to ATSR, Atmos. Meas. Tech. Discuss., 4, 2389–2431, doi:10.5194/amtd-4-2389-2011, 2011.

Rozanov, V. V., Rozanov, A. V., Kokhanovsky, A. A., and Burrows, J. P.: Radiative transfer through terrestrial atmosphere and ocean: Software package SCIATRAN, J. Quant. Spectrosc. Radiat. Transfer, 133, 13 – 71, 2014.

Sayer, A. M., Poulsen, C. A., Arnold, C., Campmany, E., Dean, S., Ewen, G. B. L., Grainger, R. G., Lawrence, B. N., Siddans, R., Thomas, G. E., and Watts, P. D.: Global retrieval of ATSR cloud parameters and evaluation (GRAPE): dataset assessment, Atmos. Chem. Phys., 11, 3913–3936, doi:10.5194/acp-11-3913-2011, 2011.

Sen, P.: Estimates of the Regression Coefficient Based on Kendall's Tau, Journal of the American Statistical Association, 63, 1379–1389, 1968.

Weber, M., Lamsal, L. N., Coldewey-Egbers, M., Bramstedt, K., and Burrows, J. P.: Pole-to-pole validation of GOME WFDOAS total ozone with groundbased data, Atmos. Chem. Phys., 5, 1341–1355, 2005.